Electronic properties of oligophenylenevinylene and oligophenyleneethynylene arrays constructed on the upper rim of a calix[4]arene core

Nicola Armaroli,*[a] Gianluca Accorsi,[a] Yannick Rio,[a] Paola Ceroni,*[b] Veronica Vicinelli,[b] Richard Welter,[c] Tao Gu,[d] Mohamed Saddik,[d] Michel Holler[d] and Jean-François Nierengarten*[d]

[a] *Laboratorio di Fotochimica, Istituto per la Sintesi Organica e la Fotoreattività, Consiglio Nazionale della Ricerche, via Gobetti 101, 40129 Bologna, Italy. E-mail: armaroli@isof.cnr.it; Fax: +39-051-6399844*
[b] *Dipartimento di Chimica "G. Ciamician", Università di Bologna, via Selmi 2, 40126 Bologna, Italy. E-mail: paola.ceroni@unibo.it*
[c] *Laboratoire DECMET, Université Louis Pasteur, 4, rue Blaise Pascal, 67000 Strasbourg, France. E-mail: welter@chimie.u-strasbg.fr*
[d] *Groupe de Chimie des Fullerènes et des Systèmes Conjugués, Ecole Européenne de Chimie, Polymères et Matériaux, Université Louis Pasteur (CNRS UMR 7504), 25 rue Becquerel, 67087 Strasbourg cedex 2, France. E-mail: jfnierengarten@chimie.u-strasbg.fr*

Heck and Sonogashira cross-coupling reactions have been used for the functionalization of the upper rim of a tetraiodinated calix[4]arene. In this way, oligophenylenevinylene (OPV) and oligophenyleneethynylene (OPE) arrays have been constructed on the calix[4]arene core to produce covalent assemblies of four π-conjugated chromophores. Electrochemical properties have been investigated by cyclic voltammetry in different solvent/electrolyte systems. Both OPV and OPE calixarenes show the simultaneous reduction of three out of four units, followed, at more negative potential, by the reduction of the fourth unit. This behaviour can be rationalized in view of a partial deconjugation in one OPV or OPE unit. On the other hand, these calixarenes show only oxidation processes corresponding to the exchange of one electron, thus demonstrating the lack of electrochemical equivalency of the OPV or OPE units, in contrast to the reduction behaviour. Electronic absorption and emission spectra have been recorded in solvents of different polarity (toluene, dichloromethane, and benzonitrile). The absorption spectra of the OPV calixarene do not match to the sum of the component units as a consequence of the partial deconjugation of the OPV arms in the calixarene structure. On the contrary, fluorescence spectra, quantum yields and excited state lifetimes of the OPV calixarene are nearly identical to those of the corresponding model compound. The trend of the absorption and emission spectra for the OPE calixarene is reversed relative to that of the OPV counterpart. Absorption spectra are well-matched with those of four trimeric OPE fragments but emission spectra exhibit, besides the typical OPE monomeric fluorescence, a broader and longer-lived emission feature on the low-energy spectral side, attributable to excimer-type interactions. Therefore the arrangement of OPV or OPE units within the same calix-4-arene skeleton brings about different effects on the electronic and luminescence properties of the multicomponent system.

Introduction

During the past decade, calix[4]arene derivatives have become increasingly important tools in host–guest chemistry.[1,2] The unique molecular architecture of these macrocyclic compounds enables the catching of ions and/or neutral guest molecules in a well-defined manner. Furthermore, several conformational isomers are possible for calix[4]arenes (cone, partial-cone, 1,2-alternate and 1,3-alternate), thus allowing the preparation of cavities with different sizes or shapes. The structural features of calix[4]arenes have also been beautifully exploited by Hosseini and co-workers for the preparation of building blocks allowing the construction of infinite networks based on co-ordination to metal ions.[3,4] In this case, the calix[4]arene core is used as a support to control the spatial orientation of the coordinating subunits. The calix[4]arene macrocycle is also an

attractive molecular scaffold for the design of new molecules combining several chromophores in a controlled spatial arrangement to study chromophore-chromophore interactions.[5–12]

Conjugated organic polymers and monomers exhibit relatively low HOMO-LUMO gaps and are potent fluorophores. This make them attractive candidates for a variety of materials science applications when semiconducting and luminescence properties are required. A leading role in this area is played by oligo- and polyphenylenevinylene (OPV and PPV) and oligo- and polyphenyleneethynylene (OPE and PPE), which have been investigated to a great extent.[13] In such systems some of the electronic/optical properties that are studied in solution are profoundly modified in the solid state. For instance, trimeric OPV molecules (3PV) are strongly luminescent in solution but exhibit weak luminescence in the solid state, due to the formation of aggregates. Chemical modification of the 3PV structure

to limit this drawback has been successfully proposed.[14] In general, although it would be convenient to transfer the knowledge acquired at the molecular level to the aggregated (solid) phase, this often turns out to be hardly feasible. Several approaches have been proposed to model the properties of solid state materials made of conjugated organic oligomers and polymers. Dendrimers decorated with OPV terminal units (up to 16) exhibit dependence of the optical properties on the dendrimer generation, suggesting intramolecular interactions.[15] A larger number of OPV units (over 2000) has been anchored to a silver nanoparticle.[16] Monolayer LB films of PPE reveal interesting structure-property relationships, indicating the crucial role played by polymer conjugation and intermolecular interactions in solid state films.[17] Another interesting approach is based on the modulation of solvent polarity in order to control aggregation phenomena of OPE and PPE in solution.[18,19]

We have recently proposed the covalent assembly of four 3PV units arising from a calix[4]arene core as a tool to investigate stacking interactions of conjugated organic molecules in dilute solution and possibly extrapolate information on electronic properties in the solid state.[12] UV-Vis absorption and electrochemical properties of our calix[4]OPV, when compared to those of a single OPV unit as reference compound, seem to indicate intramolecular electronic interactions in the calix[4]OPV array. We have also shown that the calix[4]OPV unit can act as a rigid core for the preparation of liquid crystalline derivatives.[11] In this paper, we describe the synthesis, photophysics, and electrochemistry of calix[4]OPE **2** (Scheme 1). Comparison of the electrochemical and photophysical properties of **2** with those of the corresponding calix[4]OPV analogue **1a**[11] in solution allows us to get a better picture of the electronic properties of these intriguing architectures. Notably, the absorption and luminescence properties of **1a** and **2** are remarkably different with respect to each other and also relative to the corresponding model OPV and OPE compounds. These results, along with electrochemical data, suggest that electronic properties of the calixarene architectures **1a** and **2** are affected by specific structural and conformational effects.

Results and discussion

Synthesis

The preparation of compound **1a** was achieved by following the procedure we have recently developed for the synthesis of related calix[4]OPV derivatives.[12] This synthesis is based on the functionalization of the upper rim of tetraiodinated calix[4]arene **3** (Scheme 2) with styrene derivatives under Heck conditions.

To this end, styrene **9** was prepared first (Scheme 3). Condensation of benzaldehyde **4** with aniline in refluxing benzene afforded benzaldimine **5** in 80% yield. Treatment of **5** with compound **6** under Siegrist conditions[20–22] gave stilbene **7** in 50% yield. The E stereochemistry of the double bond in **7** was confirmed by a coupling constant of *ca.* 17 Hz for the AB system, corresponding to the resonance of the vinylic protons in the ^{1}H NMR spectrum. Deprotection with CF_3CO_2H in CH_2Cl_2–H_2O, followed by reaction of the resulting **8** with methyl triphenylphosphonium bromide under Wittig conditions afforded **9** in an 80% overall yield. Calix[4]OPV **1a** was then obtained in 68% yield from **3** and **9** under Heck-type cross-coupling conditions. Compound **1a** was characterized by ^{1}H and ^{13}C NMR spectroscopy, elemental analysis and mass spectrometry. As previously observed for calix[4]OPV derivatives, **1a** gave a complicated ^{1}H NMR spectrum.[12] Actually, all the anticipated signals are present but some of them are large. This broadening suggests the existence of several conformers. Indeed, the OPV moieties in **1a** are not perpendicular to the
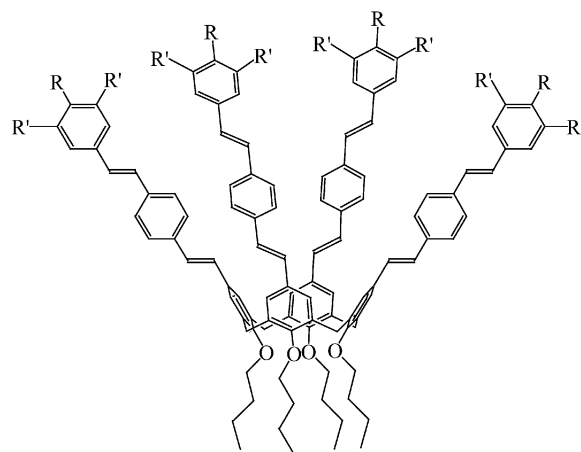

1a R = OC$_{12}$H$_{25}$, R' = H
1b R = R' = OC$_{12}$H$_{25}$
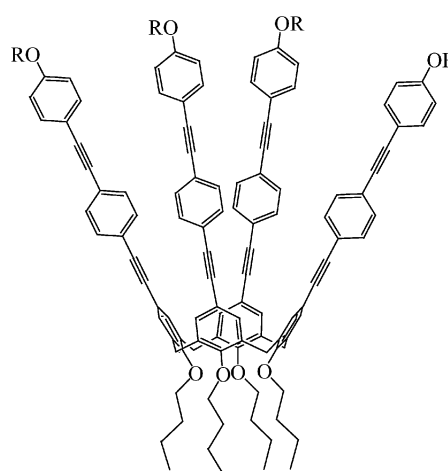

2 R = C$_{12}$H$_{25}$

Scheme 1 Calix[4]OPV derivatives **1a,b** and calix[4]OPE **2**.

calixarene core and free rotation of the four substituents on the upper rim of the calix[4]arene core is necessary to produce a NMR spectrum with sharp signals corresponding to a C_{4v} symmetrical structure. Restricted rotation in **1a** can easily be explained by steric hindering resulting from the size of the upper-rim substituents and, in good agreement with molecular modelling studies, the four OPV units may not easily accommodate simultaneously an extended planar conjugated conformation. The latter observations are quite important since they have a dramatic effect on the photophysical properties (see below). Interestingly, mesomorphic properties have been
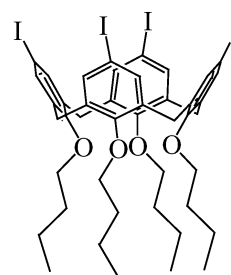

3
Scheme 2
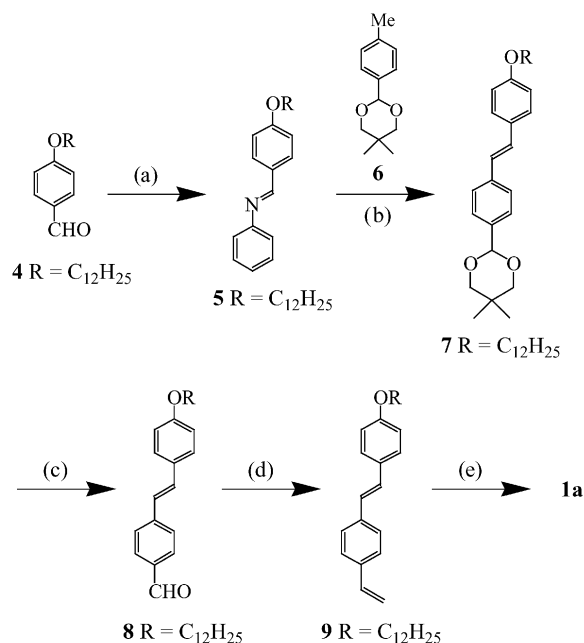
Scheme 3 Reagents and conditions: (a) aniline, C_6H_6, Δ, Dean–Stark trap, 24 h (80%); (b) t-BuOK, DMF, 80 °C, 2 h (50%); (c) CF_3CO_2H, CH_2Cl_2, H_2O, rt, 5 h (99%); (d) methyltriphenylphosphonium bromide, t-BuOK, THF, rt, 1 h (80%); (e) 3, tri-o-tolylphosphine (TOP), $Pd(OAc)_2$, Et_3N, xylene, 120 °C, 48 h (68%).

observed for compound **1a**. These have been described in detail in a preliminary communication[11] and will not be discussed herein.

The synthetic approach to prepare the calix[4]OPE derivative **2** relies upon a Sonogashira cross-coupling[23,24] reaction of a terminal alkyne derivative on the upper rim of tetraiodinated calix[4]arene **3**. The conditions for the cross-coupling reaction involving **3** were first adjusted with commercially available terminal alkynes, namely trimethylsilylacetylene and phenylacetylene (Scheme 4). The best results were obtained with $PdCl_2(PPh_3)_2$/CuI in Et_3N at room temperature. Under these conditions, reaction of **3** with an excess of trimethylsilylacetylene (10 equiv.) afforded compound **10** in 89% yield. Similarly, compound **11** was obtained in 81% yield from **3** and phenylacetylene.

The cone conformation of both **10** and **11** was deduced from their ^1H and ^{13}C NMR spectra. In particular, the ^{13}C NMR chemical shift of the methylene groups connecting the aromatic rings (δ 30.7 and 30.8 ppm for **10** and **11**, respectively) was in

10 R = SiMe₃
11 R = Ph
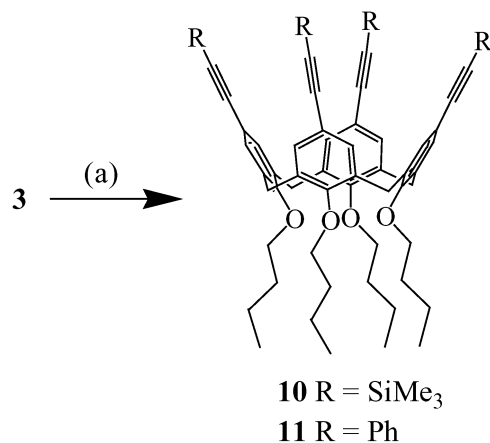
Scheme 4 Reagents and conditions: (a) trimethylsilylacetylene, $PdCl_2(PPh_3)_2$, CuI, Et_3N, rt, 72 h (**10**: 89%) or phenylacetylene, $PdCl_2(PPh_3)_2$, CuI, Et_3N, rt, 48 h (**11**: 81%).
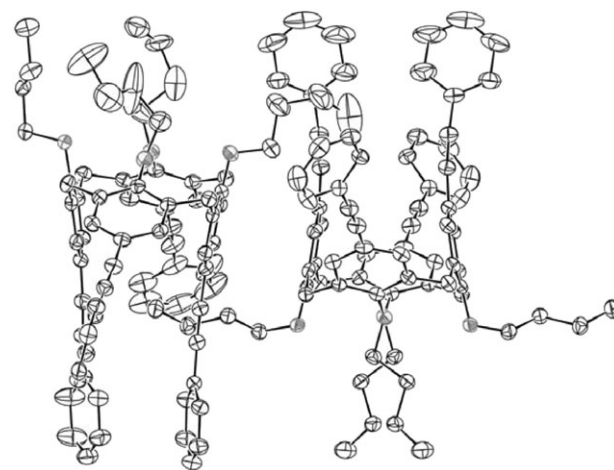

Fig. 1 ORTEP drawing of **11** showing the two conformers (left: conformer II; right: conformer V) seen in the crystal lattice.

good agreement with a cone conformation as previously shown in the literature.[25,26] For compound **11**, crystals suitable for X-ray crystal-structure analysis were obtained by slow diffusion of Et_2O into a CH_3CN–MeOH (1 : 1) solution of **11**. In the structure, two different conformers, II and V, are observed in a 2 : 1 ratio. As shown in Fig. 1, the main difference among them is the orientation of the four butyl chains as well as the orientation of the four terminal phenyl subunits. Both II and V adopt a "pinched" cone conformation in which two opposite aromatic units of the calixarene macrocycle are parallel in a face-to-face arrangement while the other two are flipped outward. Close inspection of the packing revealed a tangled array of molecules with a complicated network of intermolecular π-stacking interactions between the aromatic rings of neighbouring molecules. At the same time, the empty space resulting from the pinched cone conformation are filled with the butyl chains. The best way to describe the packing is to consider first the threesome formed by two conformers II and one conformer V (Fig. 2). Interestingly, the empty space resulting from the pinched conformation of the central V molecule is filled by one of the alkyl chains of both neighboruing II conformers. At the same time, there is a butyl unit of V located within one of the cavities of each neighbouring II molecules.

Observation of the crystal lattice down the crystallographic axis b reveals that the threesomes are arranged alternatively up and down in linear infinite chains (Fig. 3). Except for the interpenetration of the alkyl units into the cavity of neighbouring molecules to fill the voids, there are no remarkable intermolecular interactions within these linear arrays. In contrast,
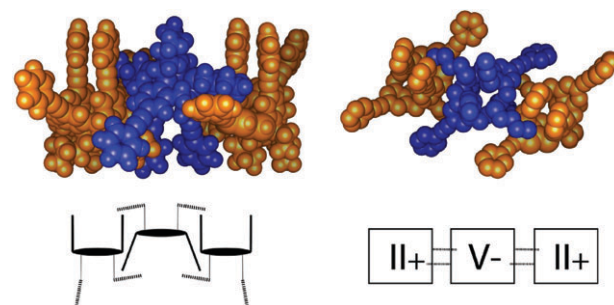

Fig. 2 Stacking within the crystal lattice of **11**: two views of the threesome formed by two conformers: II (in orange) and one conformer V (in blue). The corresponding schematic representations have been added to help the visualization; " + " indicates that the upper rim of the calixarene molecule is seen and "–" that the lower rim is seen. Molecular graphics images were produced using the UCSF Chimera package from the Computer Graphics Laboratory, University of California, San Francisco.[36]
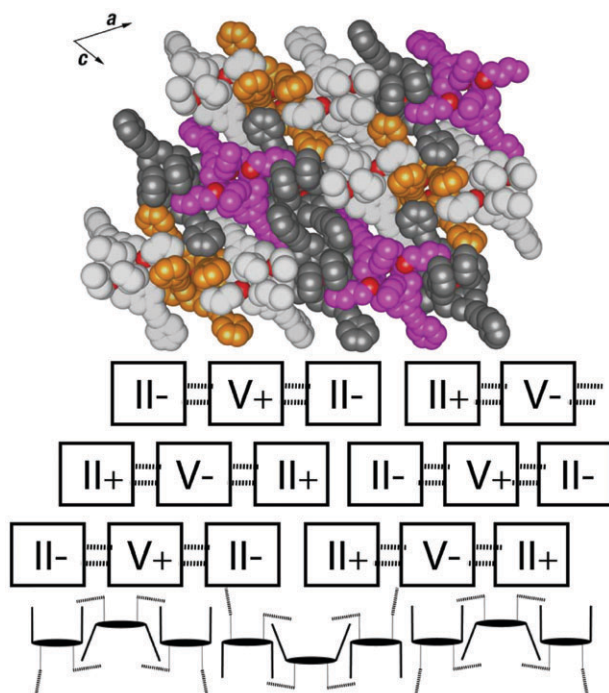
Fig. 3 Stacking within the crystal lattice of **11**: view down the crystallographic axis *b* showing the infinite parallel chains formed by the successive threesomes II–V–II arranged alternatively up and down. The corresponding schematic representations have been added to help the visualization. Molecular graphics images were produced using the UCSF Chimera package (see caption to Fig. 2).

there are several intermolecular π-π interactions between molecules belonging to neighbouring parallel chains. Interestingly, the peculiar orientation of the two central phenyl units in V can be explained by the packing forces resulting from their intermolecular π-π interactions with the phenyl moieties of two II molecules belonging each to a different neighbouring linear chain. Due to the presence of butyl groups of the other neighbouring molecules, the two central phenyl units in V cannot accommodate the face-to-face conformation observed for II but are forced to turn around to interact in an edge-to-edge manner. As a result, the bond angles at sp C atoms deviate significantly from 180°. The observed angles are effectively 169.9° and 175.5°. Additional π-π interactions can also be observed between the layers formed by the parallel linear arrays of infinite chains. The example highlighted in Fig. 4 shows how two II molecules are coupled by π-stacking interactions among successive layers. Similar pairing is also observed for the V conformers.

The preparation of the terminal alkyne **15** precursor of calix[4]OPE **2** is depicted in Scheme 5. Compound **12** was
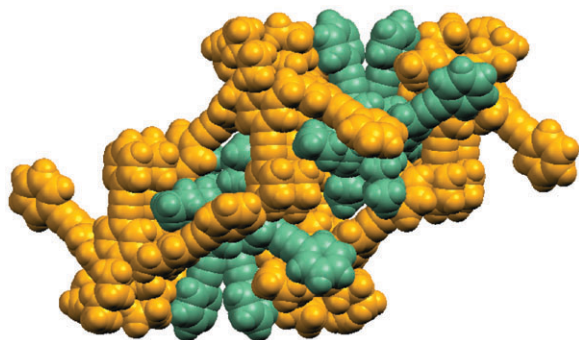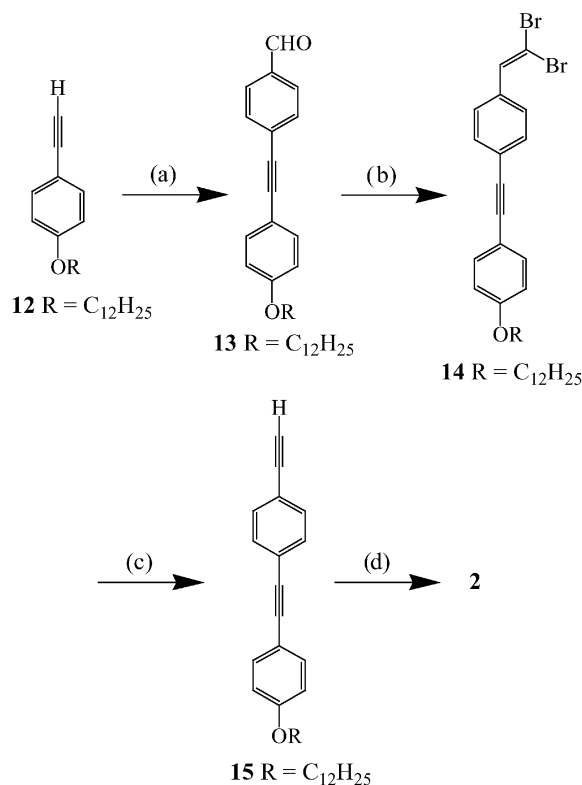

Fig. 4 Stacking within the crystal lattice of **11**: view highlighting intermolecular π-π stacking interactions. Molecular graphics images were produced using MERCURY 1.2.1 from the Cambridge Crystallographic Data Centre.[37]

Scheme 5 Reagents and conditions: (a) *p*-bromobenzaldehyde, PdCl$_2$(PPh$_3$)$_2$, CuI, Et$_3$N, rt, 72 h (70%); (b) CBr$_4$, PPh$_3$, Zn, CH$_2$Cl$_2$, 0 °C to rt, 12 h (95%); (c) LDA, THF, −70 to 0 °C, 3 h (86%); (d) **3**, PdCl$_2$(PPh$_3$)$_2$, CuI, Et$_3$N, rt, 72 h (71%).

subjected to a Pd-catalyzed cross-coupling reaction with *p*-bromobenzaldehyde to give **13** in 70% yield. Subsequent treatment with CBr$_4$/PPh$_3$/Zn under the conditions described by Corey–Fuchs[27] afforded dibromoolefin **14** in 95% yield. Elimination of HBr and halogen-metal exchange was best achieved with an excess of LDA[23,28,29] in THF at −78 °C and the resulting anion was quenched with NH$_4$Cl to give terminal alkyne **15** in 86% yield. Subsequent Sonogashira coupling with **3** gave calix[4]OPE **2** in 71% yield.

In contrast with calix[4]OPV **1a**, the ^{1}H NMR spectrum of **2** recorded at room temperature is well-resolved. In addition to the signals corresponding to the alkyloxy chains, the spectrum is characterized by a singlet for the aromatic calix[4]arene protons, two sets of AA'XX' signals for the protons of the two *p*-substituted aromatic rings and an AB quartet for the calix[4]-arene methylene groups. Clearly, the four OPE units in **2** appear equivalent in the ^{1}H NMR spectrum recorded at room temperature. However, computational studies revealed that calix[4]OPE does not adopt a regular C_{4v} symmetry, but rather a C_{2v} symmetry with a "pinched" cone conformation in which two distal OPE units are upright while the other two distal OPE units are flattened. These observations are also consistent with the X-ray crystal structure of **11** showing a "pinched" cone conformation in the solid state while its ^{1}H NMR spectrum reveals an apparent C_{4v} symmetry. Hence, as previously observed for other *O*-alkylated cone calix[4]arenes,[2] the C_{2v}–C_{2v} interconversion is faster than the NMR time scale. Therefore, the four OPE units of **2** appear equivalent. The cone conformation of **2** was further deduced from the chemical shift of the methylene groups connecting the aromatic rings (δ 30.8 ppm) in the ^{13}C NMR spectrum. Finally, the structure of **2** was also confirmed by FAB mass spectrometry showing the expected molecular ion peak at *m/z* 2187.0 (M$^+$, calculated for C$_{156}$H$_{184}$O$_8$: 2187.2). It is also worth noting that whereas liquid crystalline properties have been evidenced for calix[4]OPV **1a**,[11] the corresponding calix[4]OPE derivative **2** does not show any mesomorphic behaviour.

17 R = C$_{12}$H$_{25}$ **18** R = C$_{12}$H$_{25}$
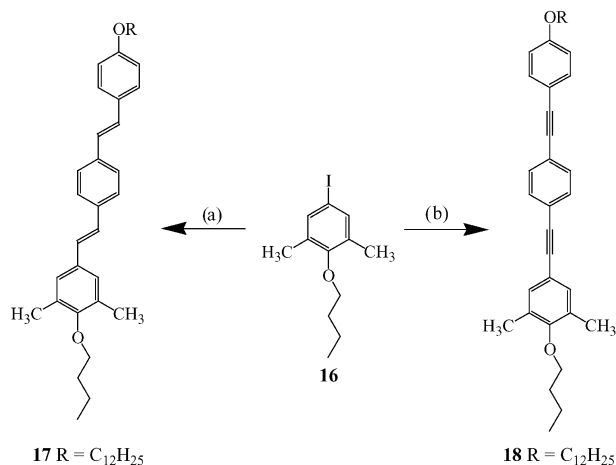
Scheme 6 Reagents and conditions: (a) **9**, TOP, Pd(OAc)$_2$, Et$_3$N, xylene, 120 °C, 48 h (89%); (b) **15**, PdCl$_2$(PPh$_3$)$_2$, CuI, Et$_3$N, rt, 24 h (80%).

The preparation of the model compounds **17** and **18** is depicted in Scheme 6. The OPV derivative **17** was obtained in 89% yield from **9** and **16** under Heck conditions. Coupling constants of *ca.* 17 Hz for the two AB systems corresponding to the two sets of vinylic protons in the ^{1}H NMR spectrum confirmed the *E* stereochemistry of both double bonds in **17**. The OPE model compound **18** was prepared in 80% yield by Pd-catalyzed cross-coupling between **15** and **16**.

Electrochemistry

The electrochemical properties of calix[4]arenes **1a** and **2** and of their model compounds, **17** and **18**, respectively, were investigated by cyclic voltammetry in different solvent/electrolyte systems. In particular, dichloromethane (DCM) was especially used to investigate the anodic potential region, while dimethylformamide (DMF) and tetrahydrofuran (THF) the cathodic one; the supporting electrolyte was tetrabutylamonium hexafluorophosphate (TBAPF$_6$) in all cases. The values of half-wave potentials ($E_{1/2}$) of the investigated compounds under different experimental conditions are gathered in Table 1.

In THF solution calix[4]arene **1a** shows two reduction processes [Fig. 5(a)]: the first one (peak I) is reversible,[30] while the second one (peak II) shows some degree of chemical

Table 1 Half-wave potentials ($E_{1/2}$ in V *vs.* SCE) of compound **1a**, **2**, **17** and **18**[a]

Compound	Solvent	Peak B	Peak A	Peak I	Peak II
1a	THF	—	—	-2.03^b	-2.35
	DMF	—	$+1.06^c$	-2.08^d	—
	DCM	$+1.09$	$+0.95$	—	—
2	DMF	—	$+1.34^c$	-2.11^b	-2.32
	DCM	—	$+1.37^c$	—	—
			$(+1.30)^d$		
17	THF	—	—	-1.98	-2.34
	DMF	—	$+1.00^c$	-2.05	—
	DCM	$+1.30$	$+1.07$	—	—
18	DMF	—	$+1.41^c$	-2.06	—
	DCM	—	$+1.46^c$	—	—
			$(+1.42)$		

[a] Cyclic voltammetry experiments at 298 K and, in parentheses, at 223 K in degassed DCM, DMF, or THF; TBAPF$_6$ as supporting electrolyte. [b] Three-electron transfer. [c] Chemically irreversible process, E_p value at 0.2 V s^{-1}. [d] Evaluation of the number of exchanged electrons is prevented by solubility problems.
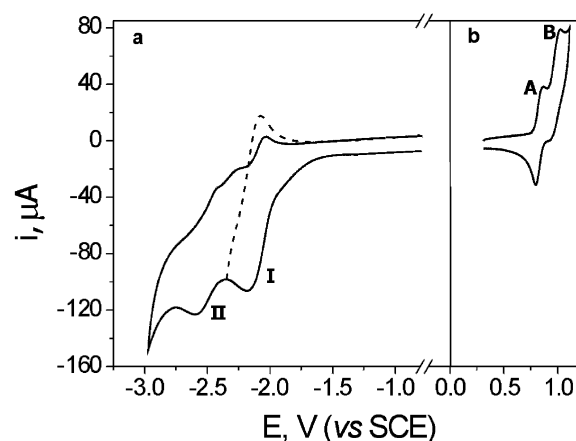

Fig. 5 Cyclic voltammogram of **1a** at room temperature in (a) THF and (b) DCM solution with TBAPF$_6$ as supporting electrolyte. $c = 0.7$ mM, $v = 0.2$ V s^{-1}.

irreversibility and the corresponding $E_{1/2}$ value was estimated by cyclic voltammograms recorded with scan rates higher than 5 V s^{-1}. The model OPV compound **17** shows two one-electron transfer processes with some degree of chemical irreversibility at potential values very close to that observed for **1a**.

Therefore, the redox processes observed for **1a** can undoubtedly be assigned to the OPV moieties, but a careful investigation was necessary to determine whether the OPV units are equivalent from an electrochemical point of view and if the dianionic form of each OPV unit can be obtained also in the calix[4]arene structure, as for the model compound **17**. The number of exchanged electrons in each redox process was estimated through chronoamperometric measurements with a Pt ultramicroelectrode ($r = 25$ µm).[31] In the case of **1a** the first reduction process corresponds to the exchange of three electrons with a slight negative shift (50 mV) compared to the model compound, while the second process involves only one electron. Therefore, the first peak is due to the simultaneous reduction of three OPV units of the calixarene, while the second one can be likely assigned to the reduction of the fourth OPV unit. Indeed, although its $E_{1/2}$ value (-2.35 V *vs.* SCE) is almost coincident with that observed for the second reduction of the OPV model compound (-2.34 V *vs.* SCE), the simultaneous presence in the calixarene of dianionic and neutral OPV units is quite unlikely.

In DCM solution both **1a** [Fig. 5(b)] and **17** show two one-electron oxidation processes, the second one (peak B) with a certain degree of chemical irreversibility. The first OPV unit is easier to oxidize ($\Delta E_{1/2} = 120$ mV) inside the calix[4]arene than
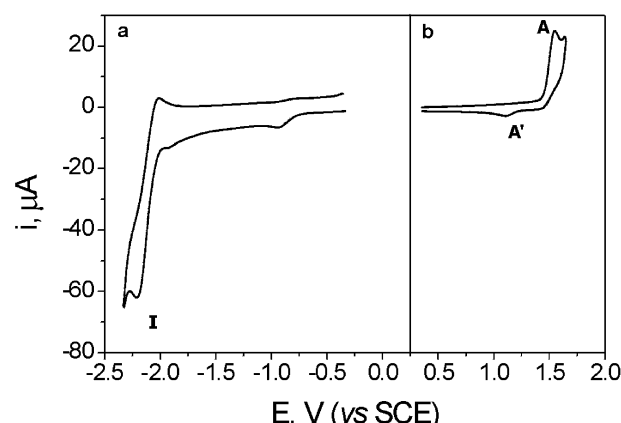

Fig. 6 Cyclic voltammogram of **2** at room temperature in (a) DMF and (b) DCM solution with TBAPF$_6$ as supporting electrolyte. $c = 0.5$ mM, $v = 0.5$ V s^{-1}. The small cathodic peak at -1 V is due to dioxygen impurities.
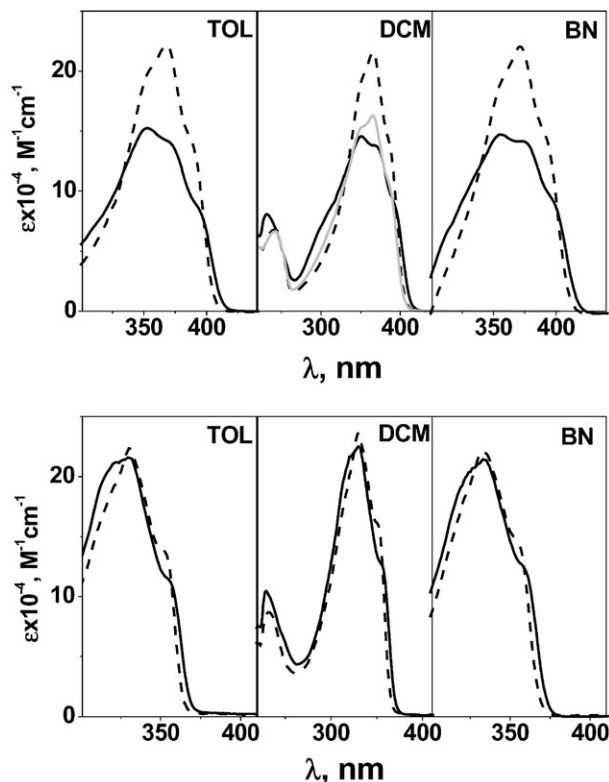
Fig. 7 Top: Absorption spectra of **1a** (—) and **17** (multiplied by a factor of 4, --). The grey profile is obtained by summing three units of **17** and one unit of an OPV dimer. Solvents: toluene (TOL), dichloromethane (DCM), and benzonitrile (BN). Bottom: Absorption spectra of **2** (—) and **18** (multiplied by a factor of 4,--).

Fig. 8 Top: Fluorescence spectra of **1a** (—) and **17** (--); λ_{exc} = 365 nm, A = 0.15. Bottom: Fluorescence spectra of **2** (—) and **18** (--); λ_{exc} = 300 nm, A = 0.15. Solvents: toluene (TOL), dichloromethane (DCM), and benzonitrile (BN), 298 K. A = Absorbance.

in the model compound. Furthermore, in the calix[4]arene **1a**, we observed the oxidation of only two out of four OPV units and these processes occur at different potentials [peaks A and B in Fig. 5(b)], thus demonstrating the lack of electrochemical equivalency of the OPV units, in contrast to the cathodic region behaviour.

The electrochemical properties of **1a** and **17** were investigated also in DMF solution: the results are similar to the previously described ones, but a quantitative discussion of the number of electrons exchanged is prevented by solubility problems.

The reduction behaviour of calix **1a** is quite different from that of the previously investigated calix **1b**.[12] The comparison of the $E_{1/2}$ values of the two calix[4]arenes shows that **1a** is significantly easier to oxidize and to reduce than the previously investigated compound, evidencing a different relative stability of the reduced and oxidized species in the two calix[4]arenes because of the presence of a different number of electron withdrawing –$OC_{12}H_{25}$ substituents. Furthermore, upon reduction, the previously investigated compound showed the electrochemical equivalency of only two OPV units: this demonstrates the influence of the long alkyl chains in determining the conformation of the calixarene structure. On the other hand, in both cases the OPV units are not equivalent from the oxidation point of view.

The same electrochemical investigations were performed for calix[4]arene **2** and its model compound **18**. The results are very similar to that of **1a**: three OPE units are reduced at the same potential [$E_{1/2}$ = −2.11 V vs. SCE, Fig. 6(a)] and the fourth one is reduced at a more negative value ($E_{1/2}$ = −2.32 V vs. SCE, not shown in Fig. 6) in DMF solution. The cyclic voltammetric experiments in THF solutions are not reported because of adsorption problems on the working electrode. In DCM solution the anodic scan of both **2** [Fig. 6(b)] and **18** shows one chemically irreversible electron transfer. Indeed, in
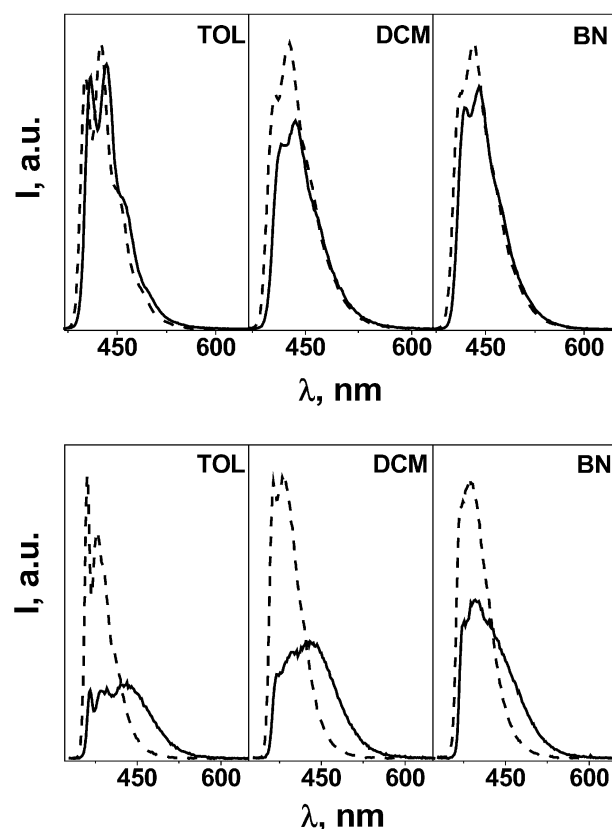
Fig. 6(b) the cathodic peak A′ is likely due to the product of the chemical reaction coupled to the first oxidation. This process attains chemical reversibility only at 223 K and scan rates higher than 1 V s$^{−1}$: the corresponding $E_{1/2}$ value of **2** is significantly positively shifted (120 mV) compared to the OPE model compound, demonstrating a higher electron-donating capability of the OPE units inside the calixarene. The number of electrons involved in the oxidation process of **2** cannot be estimated since at room temperature the peak height can be affected by the coupled chemical reaction, while at 223 K solubility problems arise.

The comparison between **1a** and **2** shows that upon reduction three out of four substituents are equivalent in both cases. This result is not in contrast with the pinched cone conformation inferred before for the neutral state, since the injection of three electrons can significantly alter the stability of the different conformations because of electrostatic repulsions. Furthermore, the OPE units of **2** are oxidized at more positive potentials than the OPV groups of **1a** and for **2** a chemical reaction is coupled to the electron transfer.

Table 2 Fluorescence band maxima and emission quantum yields at 298 K[a]

	TOL		DCM		BN	
	λ_{max}/nm	Φ_{em}	λ_{max}/nm	Φ_{em}	λ_{max}/nm	Φ_{em}
1a	434	0.84	436	0.61	440	0.85
17	426	0.93	428	0.81	432	1.00
2	432	0.22[b]	430	0.38[b]	396	0.57[b]
18	378	0.79	380	1.00	386	1.00

[a] Excitation on the absorption maximum in each case. [b] This value is rather low if compared to the other compounds and corresponds to the overall observed Φ_{em}, including excimer contribution (see Fig. 8, bottom).

Table 3 Luminescence decay times at the specified emission wavelength[a]

	TOL		DCM		BN	
	λ_{em}/nm	τ/ns	λ_{em}/nm	τ/ns	λ_{em}/nm	τ/ns
1a	450	0.9	436	1.0	450	0.9
17	450	0.8	428	1.0	450	0.9
2	366	0.8 (90%)	366	0.8 (80%)	366	0.7 (75%)
		3.5 (10%)		5.5 (20%)		5.0 (25%)
	400	0.5 (50%)	400	1.0 (63%)	400	0.8 (62%)
		3.0 (50%)		5.5 (37%)		4.7 (38%)
	480	2.9	480	5.2	480	4.6
18	366	0.7	366	0.7	366	0.7
	400	0.8	400	0.9	400	0.7

[a] λ_{exc} = 337 nm (D$_2$ lamp).

Photophysical properties

The photophysical properties of calix[4]arenes **1a** and **2**, and of their reference compounds **17** and **18**, were investigated in three solvents of different polarity, namely toluene (TOL, static dielectric constant ε = 2.4) dichloromethane (DCM, ε = 8.9), and benzonitrile (BN, ε = 25.2).

The absorption spectrum of **1a** exhibits remarkable differences (shape and intensity) from that of the reference compound **17**, whatever the solvent (Fig. 7, top). This can be attributed to ground state electronic intramolecular interactions among OPV branches or, alternatively, to partial electronic deconjugation of the π system in (some) OPV arms when assembled on the calixarene scaffold, which would result in absorption intensity decrease.[12] Interestingly, the spectrum obtained by summing *three* units of **17** and *one* unit of an OPV dimer previously reported (2PV, which corresponds to a *trans*-stilbene unit), is fairly comparable to the experimental spectrum of **1a** (Fig. 7, DCM, top). This result is somewhat in agreement with electrochemical data. The $E_{1/2}$ value for the second reduction of **1a** [−2.35 V, peak II in Fig. 5(a)] is very close to that observed for the above mentioned OPV dimer ($E_{1/2}$ = −2.34 V) in THF/TBAPF$_6$ solution. Therefore, partial deconjugation of one 3PV arm is the most likely explanation for the odd profile of the absorption spectrum.

Contrary to the trend observed for absorption spectra, the shape of the fluorescence bands of **1a** is unaffected relative to **17** (Fig. 8, top). Little emission quantum yield decrease is observed (Table 2) and the fluorescence lifetime, strictly mono-exponential, is substantially unchanged (Table 3). Excitation spectra of **1a** in any solvent are superimposable on the corresponding absorption profiles. These results are consistent with the above picture where the calixarene structure is made of three 3PV and one 2PV units and light excitation of 2PV is followed by singlet energy transfer to the 3PV units.

The absorption and luminescence spectra of the OPE calix-arene **2**, relative to the reference compound **18**, show an opposite trend relative to the OPV systems **1a** and **17**. Absorption spectra of **2** and **18** are very similar (Fig. 7, bottom), but luminescence spectra are remarkably different (Fig. 8, bottom). This trend is observed in all of the investigated solvents.

The structure of the fluorescence profile of **18** is solvent dependent and the most resolved profile is obtained in TOL. This might reflect a less pronounced distribution of OPE conformers, displaying different conjugation lengths,[17] in an apolar aromatic medium. The quantum yield of fluorescence is unitary in DCM and BN, and lower in TOL (Table 2). The excited state lifetime is very short (<1 ns) and monoexponential in any solvent, confirming that OPE-type molecules do not exhibit any anomalous luminescence behaviour, as recently pointed out by Beeby *et al.*[32] When compared to OPE **18**, the luminescence band of the calix-OPE is broadened on the low-energy side and the overall spectral shape appears to be the sum of two overlapping bands (Fig. 8, bottom). One is the regular OPE fluorescence, the other is a broader profile located at longer wavelength. The shape of the excitation spectra is independent of the emission frequency and matches the absorption profile of **18**. Thus the low-energy emission band is unambiguously assigned to intramolecular excimer-type interactions between OPE arms. Excimer emission bands have been already recorded for OPE[19] and PPE[33] aggregated systems. The lifetime decays of **2** at 298 K in the three solvents are biexponential with the shorter component (<1 ns) assigned to regular OPE fluorescence (see **18** above) and the longer component attributable to the excimer-type emission (Table 3, Fig. 9).[12]

The relative amplitude of the two decays is dependent on the emission wavelength: the longer the monitored wavelength the stronger the contribution of the longer-lived component (Table 3). Excimer-type emission tends to be favoured by increasing solvent polarity as revealed by the ratio of the lifetime relative amplitudes at 366 and 400 nm where both emission bands contribute to the observed luminescence signal. At 480 nm only the long-lived decay is monitored in all solvents (Table 3, Fig. 9). The relative intensity between monomer and excimer emission bands in **2** is concentration independent in the typical range for spectroscopic measurements, *i.e.*
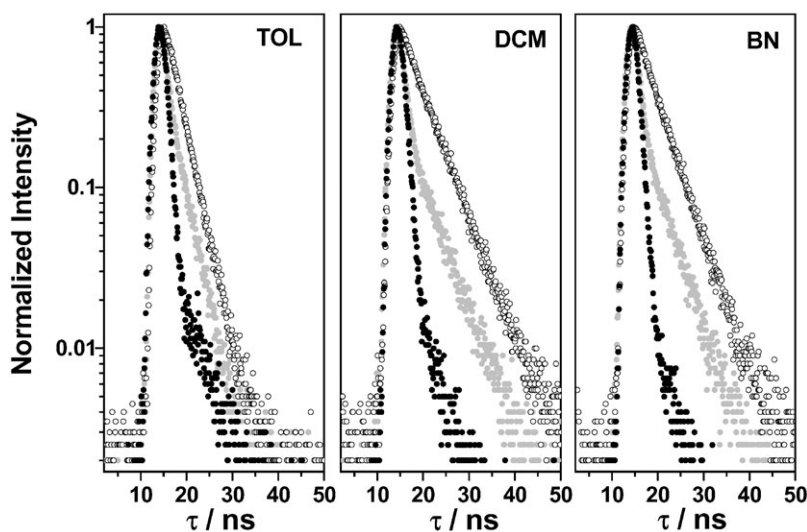

Fig. 9 Luminescence decays in TOL, DCM, and BN of **18** (black full circles) and **2** (grey full circles) at 400 nm and of **2** at 480 nm (black empty circles); λ_{exc} = 337 nm. The intermediate traces (grey full circles) evidence biexponential decays.
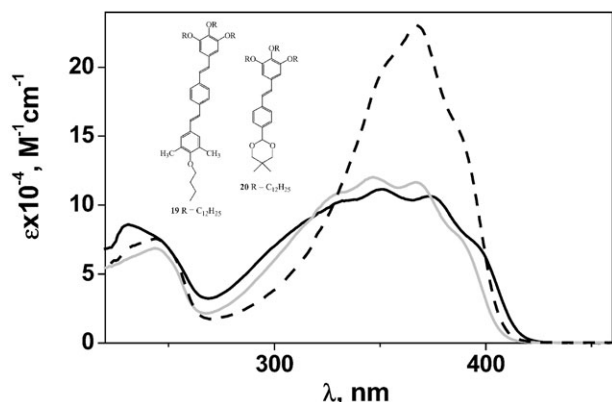
Fig. 10 Absorption spectra in DCM of **1b** (—) and its reference trimeric unit **19** (× 4, --), see ref. 12. The grey profile is obtained by summing two units of reference molecule **19** plus two units of reference molecule **20**.

10^{-7}–10^{-5} M. Therefore excimer emission is only attributable to *intra*molecular interactions occurring between the two fragments facing each other in the pinched cone conformation (see above). The fact that substantial residual monomer fluorescence is detected in all solvents indicates that a fraction of calixarene molecules cannot adopt an excited state interchromophoric distance leading to effective excimer interaction.

The opposite trends in absorption and luminescence properties of **1a** and **2** *vs.* the corresponding model compounds **17** and **18** are in line with the NMR data and the molecular modelling studies revealing differences in the average conformation between the two calixarenes (see above). Excited state interactions are observed for **2** (Fig. 8, bottom) but not for **1a** (Fig. 7, bottom). This suggests that more effective intramolecular excited state facing between calixarene branches occurs when the more rigid and linear OPE fragments are involved. There do not seem to be steric or electronic reasons as to why face-to-face interactions should be more effective for **1a** than for **2** in the ground state. Thus, partial deconjugation of some calixarene OPV branches and not ground state electronic interactions are likely to be responsible for the depressed absorption intensity of **1a** (see above).

The absorption spectrum of **1a** in DCM (λ_{max} = 350 nm, ε = 146 000 M^{-1} cm^{-1}; Fig. 7) is rather different in shape and intensity relative to that of **1b** (λ_{max} = 350 nm, ε = 111 000 M^{-1} cm^{-1}; Fig. 10).[12] Thus, steric effects induced by the long –OR terminal units may influence the calixarene conformation and OPV π conjugation. Finally, it is interesting to note that the absorption spectrum of **1b** is well-recovered by the profile obtained with *two* 3PV plus *two* 2PV residues, while a spectral comparison of **1b** with four 3PV fragments is extremely unsatisfactory, even more so than for **1a** (Fig. 10).

Conclusions

Heck and Sonogashira cross-coupling reactions were used for the successful functionalization of tetraiodinated calix[4]arene **3**. In this way, OPV and OPE arrays were constructed on the upper rim of a calix[4]arene core to produce covalent assemblies of four π-conjugated chromophores. Despite the fact that conformational flexibility might make it difficult to predict any regular trends, we emphasize the correlation between electrochemical and UV-Vis absorption for the OPV calixarenes **1a** and **1b**, which, taken in concert, seem to indicate conformational peculiarities. The absorption spectra in DCM are relatively well-matched with *three* 3PV plus *one* 2PV residues in the case of **1a**, whereas *two* 3PV plus *two* 2PV residues are found to give the best match with **1b**. In parallel the electrochemical experiments reveal that the first reduction process corresponds to three (peak I in Table 1) and two[12] equivalent 3PV units on

the calixarenes **1a** and **1b**, respectively, while the second reduction process corresponds to one and two equivalent 2PV units on **1a** and **1b**, respectively. The close vicinity of the OPV or OPE moieties in the calix[4]arene structures and the different trends of absorption, luminescence, and electrochemical properties in the two cases might provide clues on the solid state electronic properties of simple OPV and OPE chromophores.

Experimental

General methods

Reagents and solvents were purchased as reagent grade and used without further purification. THF was distilled over sodium benzophenone ketyl. Compounds **3**[12] and **16** [12] were prepared according to previously reported procedures. All reactions were performed in standard glassware under an inert Ar atmosphere. Evaporation and concentration were done at water aspirator pressure and drying *in vacuo* at 10^{-2} Torr. Column chromatography silica gel 60 (230–400 mesh, 0.040–0.063 mm) was purchased from E. Merck. Thin layer chromatography (TLC) was performed on glass sheets coated with silica gel 60 F254 purchased from E. Merck, visualization by UV light. NMR spectra were recorded on a Bruker AC 200 (200 MHz) or a Bruker AM 400 (400 MHz) with solvent peaks as reference. FAB-mass spectra (MS) were obtained on a ZA HF instrument with 4-nitrobenzyl alcohol as matrix. Elemental analyses were performed by the analytical service of the Institut Charles Sadron, Strasbourg. The molecular modelling studies have been performed on a SGI Octane^2 workstation using Spartan'02 software.

Syntheses

Compound 5. A solution of **4** (39.62 g, 139 mmol) and aniline (14.3 ml, 153 mmol) in C_6H_6 (600 ml) was refluxed for 24 h using a Dean–Stark trap. After cooling, the solution was evaporated to dryness and recrystallization (EtOH) yielded **5** (40 g, 80%) as a colourless solid (mp 61 °C). ^{1}H NMR (200 MHz, C_6D_6): 8.30 (s, 1H), 7.97 (d, J = 8 Hz, 2H), 7.34–7.10 (m, 5H), 6.94 (d, J = 8 Hz, 2H), 3.69 (t, J = 6.5 Hz, 2H), 1.75 (m, 2H), 1.50–1.30 (m, 18H), 1.04 (t, J = 6 Hz, 3H). Anal. calcd. for $C_{25}H_{35}NO$: C 82.14, H 9.65, N 3.83. Found: C 82.09, H 9.66, N 3.78.

Compound 7. *t*-BuOK (8.94 g, 75 mmol) was added to a solution of **5** (10.63 g, 29 mmol) and **6** (6.00 g, 29 mmol) in dry DMF (50 ml) under argon at 80 °C. The mixture was stirred for 2 h at 80 °C and, after cooling, poured into an aqueous 0.5 M HCl solution (500 ml). The mixture was extracted with CH_2Cl_2. The organic layer was washed with water, dried (MgSO$_4$) and evaporated to dryness. Column chromatography (SiO$_2$, hexane–CH_2Cl_2 1 : 1) gave **7** (7.02 g, 50%) as a colourless solid (mp 135 °C). ^{1}H NMR (200 MHz, CDCl$_3$): 7.49 (s, 4H), 7.44 (d, J = 8 Hz, 2H), 7.01 (AB, J = 17 Hz, 2H), 6.88 (d, J = 8 Hz, 2H), 5.40 (s, 1H), 3.97 (t, J = 6.5 Hz, 2H), 3.70 (AB, J = 11 Hz, 4H), 1.80 (m, 2H), 1.55–1.30 (m, 18H), 1.28 (s, 3H), 0.89 (t, J = 6 Hz, 3H), 0.81 (s, 3H). ^{13}C NMR (50 MHz, CDCl$_3$): 158.9, 138.2, 137.3, 129.8, 128.6, 127.7, 126.5, 126.1, 126.0, 114.7, 101.6, 77.6, 68.0, 31.9, 30.2, 29.6, 29.5, 29.4, 29.3, 26.1, 23.1, 22.7, 21.9, 14.2. Anal. calcd. for $C_{32}H_{46}O_3$: C 80.29, H 9.69. Found: C 80.21 H 9.70.

Compound 8. A mixture of **7** (2.50 g, 5.22 mmol) and CF_3CO_2H (50 ml) in CH_2Cl_2–H_2O 2 : 1 (150 ml) was stirred at rt for 5 h. The organic layer was then washed with water (3×), dried (MgSO$_4$) and evaporated to give **8** (2.03 g, 99%) as a pale yellow solid (mp 133 °C). ^{1}H NMR (200 MHz, CDCl$_3$): 8.61 (s, 1H), 7.86 (d, J = 8 Hz, 2H), 7.63 (d, J = 8 Hz, 2H),

7.48 (d, J = 8 Hz, 2H), 7.15 (AB, J = 17 Hz, 2H), 6.91 (d, J = 8 Hz, 2H), 3.99 (t, J = 7 Hz, 2H), 1.78 (m, 2H), 1.55–1.30 (m, 18H), 0.89 (t, J = 6.5 Hz, 3H). ^{13}C NMR (50 MHz, CDCl$_3$): 191.5, 159.6, 143.9, 134.9, 131.8, 130.2, 129.0, 128.2, 126.5, 124.9, 114.8, 68.1, 31.9, 29.5, 29.4, 29.3, 29.2, 26.0, 22.6, 14.1. Anal. calcd. for C$_{27}$H$_{36}$O$_2$: C 82.61, H 9.24. Found: C 82.79, H 9.36.

Compound 9. A mixture of **8** (1.90 g, 4.84 mmol), t-BuOK (0.56 g, 5.32 mmol) and methyltriphenylphosphonium bromide (1.90 g, 5.32 mmol) in dry THF (30 ml) was stirred at rt for 1 h. A saturated aqueous NH$_4$Cl solution was then added and the resulting mixture concentrated. The aqueous layer was extracted twice with CH$_2$Cl$_2$. The combined organic layers were washed with water, dried (MgSO$_4$), and evaporated to dryness. Column chromatography (SiO$_2$, hexane–CH$_2$Cl$_2$ 7 : 3) gave **9** (1.51 g, 80 %) as a pale yellow solid (mp 160 °C). ^{1}H NMR (200 MHz, CDCl$_3$) 7.48 (d, J 8 Hz, 2H), 7.41 (AB, J = 8 Hz, 4H), 7.01 (AB, J = 17 Hz, 2H), 6.89 (d, J = 8 Hz, 2H), 6.70 (dd, J = 17 and 11 Hz, 1H), 5.75 (dd, J = 17 and 2 Hz, 1H), 5.23 (d, J = 11 and 2 Hz, 1H), 3.98 (t, J = 6.5 Hz, 2H), 1.76 (m, 2H), 1.56–1.28 (m, 18H), 0.83 (t, J = 6 Hz, 3H). Anal. calcd. for C$_{28}$H$_{38}$O$_2$: C 82.71, H 9.42. Found: C 82.50, H 9.55.

Compound 1a. A mixture of **3** (300 mg, 0.26 mmol), **9** (458 mg, 1.17 mmol), TOP (6 mg) and Pd(OAc)$_2$ (3 mg) in NEt$_3$–xylene 1 : 4 (25 ml) was stirred at 120 °C under argon for 48 h. After cooling to rt, the mixture was filtered through celite (CH$_2$Cl$_2$) and evaporated. The residue was dissolved in CH$_2$Cl$_2$. The solution was washed with water (3×), dried (MgSO$_4$) and evaporated. Column chromatography (SiO$_2$, hexane–CH$_2$Cl$_2$ 1 : 1), followed by recrystallization (CH$_2$Cl$_2$–MeOH) afforded **1a** (390 mg, 68%) as a yellow solid (140 °C smectic liquid crystalline phase; 180 °C isotropic liquid). ^{1}H NMR (200 MHz, CD$_2$Cl$_2$): 7.44–6.50 (m, 56H), 4.50 (br d, J = 13 Hz, 4H), 3.90 (m, 16H), 3.24 (br d, J = 13 Hz, 4H), 1.94 (m, 8H), 1.78 (m, 8H), 1.55–1.30 (m, 80H), 1.03 (t, J = 7 Hz, 12H), 0.88 (t, J = 6.5 Hz, 12H). FAB-MS: 2203.5 (M^+ calcd. for C$_{156}$H$_{200}$O$_8$: 2203.3). Anal. calcd. for C$_{156}$H$_{200}$O$_8$: C 85.04, H 9.15. Found: C 85.39, H 8.99.

Compound 10. PdCl$_2$(PPh$_3$)$_2$ (3 mol %) and CuI (5 mol %) were added to a degassed solution of **3** (200 mg, 0.174 mmol) and trimethylsilylacetylene (0.25 ml, 1.73 mmol) in dry triethylamine (40 ml) at rt. The resulting mixture was stirred under argon at rt for 72 h, then concentrated. The residue was taken up in CH$_2$Cl$_2$. The organic layer was washed with water, dried (MgSO$_4$), filtered and evaporated. Column chromatography (SiO$_2$, hexane–CH$_2$Cl$_2$ 9 : 1) gave **10** (160 mg, 89%) as a colourless solid. ^{1}H NMR (200 MHz, CDCl$_3$): 6.94 (s, 8H), 4.35 (d, J = 13 Hz, 4H), 3.88 (t, J = 7 Hz), 3.10 (d, J = 13 Hz, 4H), 1.89 (m, 8H), 1.42 (m, 8H), 0.98 (t, J = 6.5 Hz, 12H), 0.25 (s, 36H). ^{13}C NMR (50 MHz, CDCl$_3$): 156.8, 134.3, 132.4, 116.9, 105.5, 92.7, 75.2, 32.1, 30.7, 19.3, 14.0, 0.15. Anal. calcd. for C$_{64}$H$_{88}$O$_4$Si$_4$: C 74.36, H 8.58. Found: C 74.50, H 8.45.

Compound 11. PdCl$_2$(PPh$_3$)$_2$ (3 mol %) and CuI (5 mol %) were added to a degassed solution of **3** (200 mg, 0.174 mmol) and phenylacetylene (0.2 ml, 1.74 mmol) in dry triethylamine (40 ml) at rt. The resulting mixture was stirred under argon at rt for 48 h, then concentrated. The residue was taken up in CH$_2$Cl$_2$. The organic layer was washed with water, dried (MgSO$_4$), filtered and evaporated. Column chromatography (SiO$_2$, hexane–CH$_2$Cl$_2$ 4 : 1) gave **11** (149 mg, 81%) as a colourless solid. ^{1}H NMR (200 MHz, CDCl$_3$): 7.43 (m, 8H), 7.17 (m, 12H), 6.97 (s, 8H), 4.44 (d, J = 13 Hz, 4H), 3.95 (t, J = 7 Hz), 3.19 (d, J = 13 Hz, 4H), 1.92 (m, 8H), 1.45 (m, 8H), 1.02 (t, J = 6.5 Hz, 12H). ^{13}C NMR (50 MHz, CDCl$_3$): 156.8,

134.7, 131.8, 131.5, 128.0, 127.5, 123.6, 117.1, 89.8, 88.1, 75.1, 32.2, 30.8, 19.3, 14.0. Anal. calcd. for C$_{76}$H$_{72}$O$_4$: C 86.99, H 6.92. Found: C 86.86, H 6.99.

Compound 13. PdCl$_2$(PPh$_3$)$_2$ (3 mol %) and CuI (5 mol %) were added to a stirred degassed solution of **12** (4.30 g, 15 mmol) and 4-bromobenzaldehyde (4.16 g, 22.5 mmol) in dry triethylamine (40 ml) at rt. The resulting mixture was stirred at rt for 48 h, then concentrated. The residue was taken up in CH$_2$Cl$_2$. The organic layer was washed with water, dried (MgSO$_4$), filtered and evaporated. Column chromatography (SiO$_2$, hexane–CH$_2$Cl$_2$ 7 : 3) gave **13** (4.10 g, 70%) as a colourless solid glassy product. ^{1}H NMR (200 MHz, CDCl$_3$): 8.58 (s, 1H), 7.86 (d, J = 8 Hz, 2H), 7.65 (d, J = 8 Hz, 2H), 7.49 d, J = 8 Hz, 2H), 6.89 (d, J = 8 Hz, 2H), 3.98 (t, J = 6.5 Hz, 2H), 1.77 (m, 2H), 1.60–1.30 (m, 18H), 0.89 (t, J = 6.5 Hz, 3H). ^{13}C NMR (50 MHz, CDCl$_3$): 191.3, 159.7, 135.0, 133.3, 131.8, 130.0, 129.5, 114.6, 114.2, 93.9, 87.4, 68.1, 31.9, 29.6, 29.5, 29.3, 29.1, 25.9, 22.6, 14.1. Anal. calcd. for C$_{27}$H$_{34}$O$_2$: C 83.03, H 8.77. Found: C 83.29, H 8.99.

Compound 14. A mixture of CBr$_4$ (17.18 g, 51.8 mmol), PPh$_3$ (13.64 g, 51.8 mmol) and Zn dust (3.39 g, 51.8 mmol) in dry CH$_2$Cl$_2$ (200 ml) was stirred at rt for 24 h. The suspension was then cooled to 0 °C and a solution of **13** (4.05 g, 10.37 mmol) in CH$_2$Cl$_2$ (30 ml) was added at once. The resulting mixture was slowly warmed up to rt (1 h) and stirred at this temperature overnight. The resulting thick suspension was filtered over SiO$_2$ (CH$_2$Cl$_2$) to remove the zinc salts and some of the P-containing by-products. The solution was concentrated and column chromatography (SiO$_2$, CH$_2$Cl$_2$–hexane 1 : 1) gave **14** (5.4 g, 95%) as colourless glassy product. ^{1}H NMR (200 MHz, CDCl$_3$): 7.50 (AB, J = 8 Hz, 4H), 7.47 (s, 1H), 7.45 (d, J = 8 Hz, 2H), 6.85 (d, J = 8 Hz, 2H), 3.97 (t, J = 6.5 Hz, 2H), 1.77 (m, 2H), 1.60–1.30 (m, 18H), 0.89 (t, J = 6.5 Hz, 3H). ^{13}C NMR (50 MHz, CDCl$_3$): 159.4, 136.2, 134.5, 133.0, 131.3, 128.3, 123.9, 114.5, 92.3, 91.0, 90.0, 87.7, 68.1, 31.9, 29.6, 29.5, 29.4, 29.2, 26.0, 22.7, 14.1. Anal. calcd. for C$_{28}$H$_{34}$OBr$_2$: C 61.55, H 6.27. Found: C 61.52, H 6.36.

Compound 15. A 2.0 M solution of LDA in THF (30 ml, 60 mmol) was added dropwise to a solution of **14** (5.35 g, 9.79 mmol) in dry THF (120 ml) at −78 °C under argon. The resulting was stirred for 2 h at −78 °C, then allowed to warm up to 0 °C (1 h) and a saturated aqueous NH$_4$Cl solution (60 ml) was added. The mixture was then diluted with hexane. The organic layer was washed with H$_2$O (2×), dried (MgSO$_4$), filtered and evaporated. Column chromatography (SiO$_2$, hexane–CH$_2$Cl$_2$ 7 : 3) gave **15** (3.25 g, 86%) as pale yellow glassy product. ^{1}H NMR (200 MHz, CDCl$_3$): 7.46 (d, J = 8 Hz, 2H), 7.45 (s, 4H), 6.87 d, J = 8 Hz, 2H), 3.97 (t, J = 6.5 Hz, 2H), 3.16 (s, 1H), 1.78 (m, 2H), 1.55–1.30 (m, 18H), 0.88 (t, J = 6.5 Hz, 3H). ^{13}C NMR (50 MHz, CDCl$_3$): 159.4, 136.2, 133.1, 132.0, 131.2, 128.3, 124.2, 121.4, 114.7, 114.5, 91.6, 87.5, 83.3, 78.7, 68.0, 31.9, 29.7, 29.6, 29.4, 29.2, 26.0, 22.7, 14.1. Anal. calcd. for C$_{28}$H$_{34}$O: C 87.00, H 8.86. Found: C 86.88, H 9.01.

Compound 2. PdCl$_2$(PPh$_3$)$_2$ (3 mol %) and CuI (5 mol %) were added to a degassed solution of **3** (100 mg, 0.087 mmol) and **15** (325 mg, 0.87 mmol) in dry triethylamine (40 ml) at rt. The resulting mixture was stirred under argon at rt for 48 h, then concentrated. The residue was taken up in CH$_2$Cl$_2$. The organic layer was washed with water, dried (MgSO$_4$), filtered and evaporated. Column chromatography (SiO$_2$, hexane–CH$_2$Cl$_2$ 4 : 1) gave **2** (135 mg, 71%) as a pale yellow solid (mp 126 °C). ^{1}H NMR (400 MHz, CD$_2$Cl$_2$): 7.41 (d, J = 8 Hz, 8H), 7.36 (AB, J = 8 Hz, 16H), 6.97 (s, 8H), 6.77 (d, J = 8 Hz, 8H), 4.52 (d, J = 13 Hz, 4H), 3.99 (t, J = 6.5 Hz, 8H), 3.97

(t, J = 6.5 Hz, 8H), 3.21 (d, J = 13 Hz, 4H), 1.97 (m, 8H), 1.81 (m, 8H), 1.58–1.29 (m, 80H), 1.03 (t, J = 6.5 Hz, 12H), 0.90 (t, J = 6.5 Hz, 12H). ^{13}C NMR (50MHz, CDCl$_3$): 159.1, 157.0, 134.7, 133.0, 131.8, 131.2, 131.1, 122.9, 122.8, 116.8, 115.0, 114.4, 91.5, 91.0, 88.1, 88.0, 75.1, 68.0, 32.2, 31.9, 30.8, 29.6, 29.4, 29.3, 29.2, 26.0, 22.7, 19.3, 14.1, 14.0. FAB-MS: 2187.0 (M^+, calcd. for C$_{156}$H$_{184}$O$_8$: 2187.2). Anal. calcd. for C$_{156}$H$_{184}$O$_8$: C 85.67, H 8.48. Found: C 85.68, H 8.27.

Compound 17. A mixture of **16** (300 mg, 1.07 mmol), **9** (435 mg, 1.07 mmol), TOP (25 mg) and Pd(OAc)$_2$ (10 mg) in NEt$_3$– xylene 1 : 4 (25 ml) was stirred at 120 °C under argon for 48 h. After cooling to rt, the mixture was filtered through celite (CH$_2$Cl$_2$) and evaporated. The residue was dissolved in CH$_2$Cl$_2$. The solution was washed with water (3×), dried (MgSO$_4$) and evaporated. Column chromatography (SiO$_2$, hexane–CH$_2$Cl$_2$ 2 : 1 to 1 : 1) afforded **17** (540 mg, 89%) as a pale yellow solid (110 °C smectic C liquid crystalline phase; 149 °C smectic A liquid crystalline phase; 154 °C nematic liquid crystalline phase; 181 °C isotropic liquid). ^{1}H NMR (200 MHz, CDCl$_3$): 7.47 (s, 4H), 7.43 (d, J = 8 Hz, 2H), 7.19 (s, 2H), 7.03 (AB, J = 17 Hz, 2H), 7.01 (AB, J = 17 Hz, 2H), 6.90 (d, J = 8 Hz, 2H), 3.98 (t, J = 6.5 Hz, 2H), 3.78 (t, J = 6.5 Hz, 2H), 2.31 (s, 6H), 1.80 (m, 4H), 1.60–1.30 (m, 20H), 1.01 (t, J = 6.5 Hz, 3H), 0.89 (t, J = 6.5 Hz, 3H). ^{13}C NMR (50MHz, CDCl$_3$): 158.9, 155.9, 136.7, 136.5, 133.0, 132.6, 131.1, 129.9, 128.0, 127.6, 127.0, 126.9, 126.5, 126.5, 126.0, 114.7, 72.1, 68.0, 32.5, 31.8, 29.6, 29.5, 29.4, 29.3, 26.0, 22.6, 19.3, 16.3, 14.1, 13.9, Anal. calcd. for C$_{40}$H$_{54}$O$_2$: C 84.75, H 9.60. Found: C 84.62 H 9.39.

Compound 18. PdCl$_2$(PPh$_3$)$_2$ (3 mol %) and CuI (5 mol %) were added to a degassed solution of **16** (200 mg, 0.658 mmol) and **15** (254 mg, 0.658 mmol) in dry triethylamine (15 ml) at rt. The resulting mixture was stirred under argon at rt for 24 h, then concentrated. The residue was taken up in CH$_2$Cl$_2$. The organic layer was washed with water, dried (MgSO$_4$), filtered and evaporated. Column chromatography (SiO$_2$, hexane– CH$_2$Cl$_2$ 4 : 1) gave **2** (300 mg, 80%) as a pale yellow solid (mp 128 °C). ^{1}H NMR (200 MHz, CDCl$_3$): 7.46 (s, 4H), 7.44 (d, J = 8 Hz, 2H), 7.21 (s, 2H), 6.88 (d, J = 8 Hz, 2H), 3.98 (t, J = 6.5 Hz, 2H), 3.78 (t, J = 6.5 Hz, 2H), 2.28 (s, 6H), 1.78 (m, 4H), 1.60–1.28 (m, 20H), 1.00 (t, J = 6.5 Hz, 3H), 0.89 (t, J = 6.5 Hz, 3H). ^{13}C NMR (50 MHz, CDCl$_3$): 159.4, 156.6, 133.0, 132.1, 131.3, 131.2, 123.2, 123.0, 118.0, 114.8, 114.5, 91.3, 91.2, 88.0, 87.8, 72.1, 68.0, 32.4, 31.9, 31.6, 29.6, 29.6, 29.3, 29.2, 29.0, 26.9, 26.0, 22.6, 19.3, 16.1, 14.1, 13.9. Anal. calcd. for C$_{40}$H$_{50}$O$_2$: C 85.36, H 8.95. Found: C 85.47, H 8.79.

Crystal structure determination of 11

The colourless crystal used for the diffraction study was produced by slow diffusion of Et$_2$O into a CH$_3$CN–MeOH (1 : 1) solution of **11**. Diffraction data were collected on a Kappa CCD diffractometer using graphite-monochromated MoKα radiation (λ = 0.710 73 Å). Data were collected using phi- scans and the structures were solved by direct methods using SHELX97 software[38] and the refinements were conducted by full-matrix least squares on F^2. No absorption correction was used. All non-hydrogen atoms were refined anisotropically. Hydrogen atoms were generated according to stereochemistry and refined using a riding model in SHELXL97. Half of an H$_2$O molecule has to be considered to explain the low electronic residual (≈ 2 e$^-$ Å^{-3}).†

Electrochemistry

The electrochemical experiments were carried out in argon-purged DCM, DMF (Romil Hi-Dry™) or THF (Aldrich) solutions at 298 or 223 K with an EcoChemie Autolab 30 multipurpose instrument interfaced to a personal computer. In cyclic voltammetry (CV) the working electrode was a glassy carbon electrode (0.08 cm^2, Amel) or a Pt disk ultramicroelectrode (r = 25 µm). In all cases, the counter electrode was a Pt spiral, separated from the bulk solution with a fine glass frit, and a silver wire was employed as a quasi-reference electrode (AgQRE). The potentials reported are referred to SCE by measuring the AgQRE potential with respect to ferrocene. The concentration of the compounds examined was of the order of 5×10^{-4} M; 0.05 M tetrabuthylammonium hexafluorophosphate (TBAPF$_6$) was added as supporting electrolyte. Cyclic voltammograms were obtained with scan rates in the range 0.05–20 V s^{-1}. The CV simulations were carried out by the DIGISIM program. The diffusion coefficients and the number of electrons exchanged in each electron transfer process were determined by chronoaperometric experiments performed with a Pt disk ultramicroelectrode (r = 25 µm) by the method reported by Bard *et al.*[31]

Photophysics

The photophysical investigations were carried out in CH$_2$Cl$_2$ and toluene (Carlo Erba, spectrofluorimetric grade), and in benzonitrile (Aldrich, HPLC grade). The samples were placed in fluirimetric 1 cm path cuvettes. Absorption spectra were recorded with a Perkin–Elmer l40 spectrophotometer. Uncorrected emission spectra were obtained with a Spex Fluorolog II spectrofluorimeter (continuous 150 W Xe lamp), equipped with a Hamamatsu R-928 photomultiplier tube. The corrected spectra were obtained *via* a calibration curve. Fluorescence quantum yields obtained from spectra on an energy scale (cm^{-1}) were measured with the method described by Demas and Crosby[34] using as standards air-equilibrated solutions of quinine sulfate in 1 N H$_2$SO$_4$ (Φ_{em} = 0.546).[35] To record the 77 K luminescence spectra, the samples were put in glass tubes (2 mm diameter) and inserted in a special quartz dewar, filled up with liquid nitrogen. Emission lifetimes on the nanosecond time scale were determined with an IBH single-photon-counting spectrometer equipped with a thyratron gated nitrogen lamp working in the range 2–40 kHz (λ_{exc} = 337 nm, 0.5 ns time resolution); the detector was a red-sensitive (185–850 nm) Hamamatsu R-3237-01 photomultiplier tube. Experimental uncertainties are estimated to be 8% for lifetime determinations, 20% for emission quantum yields, and 1 nm and 5 nm for absorption and emission peaks, respectively.

References

1 J. Vicens and V. Bohmer, *Calixarenes: A Versatile Class of Macrocyclic Compounds*, Kluwer Academic Publishers, Dordrecht, The Netherlands, 1991.
2 A. Ikeda and S. Shinkai, *Chem. Rev.*, 1997, **97**, 1713.
3 H. Akdas, E. Graf, M. W. Hosseini, A. De Cian and J. M. Harrowfield, *Chem. Commun.*, 2000, 2219.

4   H. Akdas, E. Graf, M. W. Hosseini, A. De Cian, A. Bilyk, B. W. Skelton, G. A. Koutsantonis, I. Murray, J. M. Harrowfield and A. H. White, *Chem. Commun.*, 2002, 1042.
5   H. Matsumoto and S. Shinkai, *Chem. Lett.*, 1994, 2431.
6   H. Matsumoto and S. Shinkai, *Tetrahedron Lett.*, 1996, **37**, 77.
7   G. P. Bartholomew and G. C. Bazan, *Acc. Chem. Res.*, 2001, **34**, 30.
8   S. J. Wang, W. J. Oldham, R. A. Hudack and G. C. Bazan, *J. Am. Chem. Soc.*, 2000, **122**, 5695.
9   S. J. Wang, G. C. Bazan, S. Tretiak and S. Mukamel, *J. Am. Chem. Soc.*, 2000, **122**, 1289.
10 M. R. Robinson, S. J. Wang, G. C. Bazan and Y. Cao, *Adv. Mater.*, 2000, **12**, 1701.
11 T. Gu, G. Accorsi, N. Armaroli, D. Guillon and J. F. Nierengarten, *Tetrahedron Lett.*, 2001, **42**, 2309.
12 T. Gu, P. Ceroni, G. Marconi, N. Armaroli and J. F. Nierengarten, *J. Org. Chem.*, 2001, **66**, 6432.
13 K. Müllen and G. Wegner, *Electronic Materials: The Oligomer Approach*, Wiley–VCH, Weinheim, 1998.
14 F. He, G. Cheng, H. Q. Zhang, Y. Zheng, Z. Q. Xie, B. Yang, Y. G. Ma, S. Y. Liu and J. C. Shen, *Chem. Commun.*, 2003, 2206.
15 S. C. J. Meskers, M. Bender, J. Hubner, Y. V. Romanovskii, M. Oestreich, A. Schenning, E. W. Meijer and H. Bassler, *J. Phys. Chem. A*, 2001, **105**, 10220.
16 F. Stellacci, C. A. Bauer, T. Meyer-Friedrichsen, W. Wenseleers, S. R. Marder and J. W. Perry, *J. Am. Chem. Soc.*, 2003, **125**, 328.
17 J. Kim, I. A. Levitsky, D. T. McQuade and T. M. Swager, *J. Am. Chem. Soc.*, 2002, **124**, 7710.
18 C. E. Halkyard, M. E. Rampey, L. Kloppenburg, S. L. Studer-Martinez and U. H. F. Bunz, *Macromolecules*, 1998, **31**, 8655.
19 C. Y. Tan, M. R. Pinto and K. S. Schanze, *Chem. Commun.*, 2002, 446.
20 A. E. Siegrist, P. Liechti, H. R. Meyer and K. Weber, *Helv. Chim. Acta*, 1969, **52**, 2521.
21 G. Zerban and H. Meier, *Z. Naturforsch., B: Chem. Sci.*, 1993, **48**, 171.
22 A. Skibniewski, G. Bluet, N. Druze and O. Riant, *Synthesis*, 1999, 459.
23 T. Gu and J. F. Nierengarten, *Tetrahedron Lett.*, 2001, **42**, 3175.
24 K. Sonogashira, in *Metal-catalyzed Cross-coupling Reactions*, eds. F. Diederich and P. Stang, Wiley–VCH, Weinheim, Germany, 1998, p. 203.
25 C. Jaime, J. Demendoza, P. Prados, P. M. Nieto and C. Sanchez, *J. Org. Chem.*, 1991, **56**, 3372.
26 J. B. Regnouf de Vains and R. Lamartine, *Tetrahedron Lett.*, 1996, **37**, 6311.
27 E. J. Corey and P. L. Fuchs, *Tetrahedron Lett.*, 1972, **13**, 3769.
28 J. F. Nierengarten, M. Schreiber, F. Diederich and V. Gramlich, *New J. Chem.*, 1996, **20**, 1273.
29 N. Solladié and M. Gross, *Tetrahedron Lett.*, 1999, **40**, 3359.
30 A fully reversible process is observed upon reversing the scan potential right after peak I, as shown by the dashed line in Fig. 5(a).
31 G. Denuault, M. V. Mirkin and A. J. Bard, *J. Electroanal. Chem.*, 1991, **308**, 27.
32 A. Beeby, K. Findlay, P. J. Low and T. B. Marder, *J. Am. Chem. Soc.*, 2002, **124**, 8280.
33 H. Li, D. R. Powell, R. K. Hayashi and R. West, *Macromolecules*, 1998, **31**, 52.
34 J. N. Demas and G. A. Crosby, *J. Phys. Chem.*, 1971, **75**, 991.
35 S. R. Meech and D. Phillips, *J. Photochem.*, 1983, **23**, 193.
36 C. C. Huang, G. S. Couch, E. F. Pettersen and T. E. Ferrin, in *Pacific Symposium on Biocomputing*, 1996, vol. **1**, p. 724.
37 I. J. Bruno, J. C. Cole, P. R. Edgington, M. K. Kessler, C. F. Macrae, P. McCabe, J. Pearson and R. Taylor, *Acta Crystallogr., Sect. B*, 2002, **58**, 389.
38 *Kappa CCD Operation Manual*, Nonius B.V., Delft, The Netherlands, 1997G. M. Sheldrick, *SHELXL-97, Program for refinement of crystal structures*, University of Göttingen, Germany, 1997.